Journal of the Optical Society of America B

OPTICAL PHYSICS

Enhancement of squeezing with cascaded and coherent feedback-controlled degenerate optical parametric amplifiers

Yashuai Han,[1,4] Zhao Zhang,[1] Zhengxian Zhou,[1] Jun Qu,[1] Jun He,[2,3] and Junmin Wang[2,3,5]

[1]Anhui Province Key Laboratory of Photo-Electronic Materials Science and Technology, and College of Physics and Electronic Information, Anhui Normal University, Wuhu, Anhui 241000, China
[2]State Kay Laboratory of Quantum Optics and Quantum Optics Devices, and Institute of Opto-Electronics, Shanxi University, Taiyuan, Shanxi 030006, China
[3]Collaborative Innovation Center of Extreme Optics, Shanxi University, Taiyuan, Shanxi 030006, China
[4]e-mail: 594362444@qq.com
[5]e-mail: wwjjmm@sxu.edu.cn

Received 2 August 2021; revised 28 August 2021; accepted 31 August 2021; posted 2 September 2021 (Doc. ID 439467); published 28 September 2021

The squeezing level of light on atomic resonance produced by a degenerate optical parametric amplifier (DOPA) is now limited by blue or violet pump-light-induced loss, and it is difficult to improve the squeezing by simply reducing the loss of DOPA. In this study, two promising schemes, namely, the cascaded DOPA (C-DOPA) and the coherent feedback-controlled DOPA (CFC-DOPA), are theoretically discussed. For a ideal case, the CFC-DOPA can realize infinite squeezing output but requires almost infinite accuracy in phase locking. For a practical case with feasible physical parameters of realistic systems, the performance of squeezing enhancement for the C-DOPA and CFC-DOPA is compared. The C-DOPA shows advantages in the megahertz frequency range, while the CFC-DOPA shows advantages in the low-frequency range. At a general analysis frequency of 2 MHz, C-DOPA shows better robustness against the loss of the system. As a price, it requires a smaller instability tolerance for phase locking. With the C-DOPA, the squeezing on Rb atomic resonance can be pushed from −5 dB to −7 dB. Our analytical results can provide a valuable reference for designing experimental devices to efficiently produce high-quality squeezed light on atomic resonance, which has potential applications in quantum information processing and quantum metrology.

https://doi.org/10.1364/JOSAB.439467

1. INTRODUCTION

Squeezed light is an essential resource for quantum information processing [1], quantum computation [2,3], and quantum precision measurements [4,5]. Thus far, several approaches have been developed for the production of squeezed light, including four-wave mixing based on the third-order nonlinearity of atomic ensembles [6–9], optical parametric oscillators (OPOs) based on the second-order nonlinearity of nonlinear crystals [10–14], and optical fibers based on the third-order Kerr type nonlinearity [15,16]. Recently, benefiting from the development of nonlinear crystal fabrication technology and optical coating technology, the squeezing level produced by the OPO has been significantly improved [11–14], and a maximum squeezing degree of −15 dB has been achieved [12], proving that the OPO is one of the most effective approaches. However, these results mainly focused on the near-infrared or infrared bands, for example, 1.06 μm and 1.5 μm.

With the rapid development of atomic physics, the interaction between light and atoms has become a major concern. The squeezed light corresponding to the transitions of alkali metal atoms, such as Cs and Rb, has significant potential for application in the construction of practical quantum networks [17], improvement of the sensitivity of atomic noise spectroscopy [18,19], and atomic optical magnetometers [20]. The squeezed light near or on atomic resonance has been produced based on the OPO and the four-wave mixing in an atomic vapor cell. Besides the two schemes, the polarization self-rotation in an atomic vapor cell is also another suitable candidate. Based on the four-wave mixing in an atomic vapor, an efficient intensity difference squeezing of −9 dB when operating off resonance with Rb atomic transitions has been produced [21–23], and −6.3 dB for single resonance with Rb atomic transitions has been observed [9]. With the same scheme, an intensity difference squeezing of −6.5 dB also for single resonance near Cs atomic resonance was obtained [24]. However, the maximum single-mode squeezing obtained in experiments with four-wave mixing [7,8] and polarization self-rotation [25–27] is only −4 dB and −3 dB, and the squeezing level seriously depends on the detuning of atomic transitions. The OPO is free of this, which can produce subequal single-mode squeezing near atomic resonance. With the OPO, numerous groups [28–33] have realized single-mode squeezed light corresponding to atomic transitions in experiments. Takeno *et al.* achieved effective squeezing of −9 dB at 860 nm [28]; however, it was detuned from the Cs D_2 line for several nanometers. Burks *et al.* [29] and Tian *et al.* [30] obtained −3.0 dB and −3.5 dB of squeezing at 852 nm, resonant to the Cs D_2 line. For the D_1 line of Rb, considerable efforts have been made to improve the squeezing level. Tanimura *et al.*, Wolfgramm *et al.*, and Hétet *et al.* reported the squeezing of −2.75 dB [31], −3.5 dB [20], and −5.2 dB [32] at 795 nm, respectively. In 2016, our group improved the squeezing degree to −5.6 dB [33], which is the highest squeezing level reported at the D_1 line of Rb.

It can be seen from the above that the observed squeezing level on atomic resonance is quite limited compared with the results at 1.06 μm and 1.5 μm. The intrinsic limiting factor is that the wavelengths of the atomic transitions are short. The squeezing of lights is quite sensitive to its loss. With the shortening of the wavelength, the absorption losses of both the nonlinear crystals and the mirrors strengthen. For 1.06 μm and 1.5 μm, the loss of the OPO cavity can be lower than 0.1% [12,13], which is quite difficult to achieve for the OPO on atomic transitions. At present, the intracavity loss of the OPO at 795 nm reported in the published papers [31–33] is approximately 0.5%. In addition, the OPO needs to be pumped by the beam at the harmonic wavelengths, which is mainly in the blue or violet band for the wavelengths of atomic transitions. The blue or violet pump beam induces a loss increase of the nonlinear crystals for the fundamental beam owing to the blue-induced infrared absorption [34] and the gray-tracking effect [32,35]. This effect becomes quite serious when the wavelength shortens to 795 nm, and exposure to a violet laser with high power may cause damage to the crystals. To avoid this, Hétet *et al.* recommended restricting the power of 398 nm to 50 mW [32]. To ensure the tenability of the wavelength, the OPO at these wavelengths is designed to only resonate with the signal light, resulting in higher threshold power. Therefore, for the production of squeezed light at 795 nm, OPO is operated at a moderate normalized pump parameter, which also limits the output squeezing level. The additional losses and moderate pump parameter together lead to the fact that the squeezing level on atomic resonance is far below the record of 15 dB at 1.06 μm.

In some practical application scenarios [17–20], the phase of the squeezed light should be controlled. Although the phase of the squeezed vacuum state can be locked with the scheme of quantum noise locking [36], the stability of phase locking is significantly less than that achieved with traditional coherent modulation locking. Hence, the quadrature squeezed light possessing coherent components enables the realization of stable phase locking. By injecting a signal beam into the OPO and running it as a degenerate optical parametric amplifier (DOPA), one can obtain quadrature squeezed light. At the 795 nm Rb D_1 line, the squeezing of the quadrature squeezed light produced in the experiment is limited to −4.0 dB [32]. For a wavelength authentically resonant to the Cs D_2 line, the squeezing level is also at this level [29,30]. The low squeezing level limits the application potential in actual quantum information processing and quantum metrology. To enhance the squeezing level output from the DOPA with the practical loss and pump parameters, two feasible schemes are applied: cascaded DOPA (C-DOPA) [37,38] and coherent feedback-controlled DOPA (CFC-DOPA) [39–42]. TheC-DOPA denotes a system that seeds the squeezed light generated by one DOPA into the other DOPA, while the CFC-DOPA is a system that feeds the squeezed light produced by the DOPA back into the input port. Both schemes have been proven to have the ability to enhance the squeezing [37–42]. The production of quadrature entangled light with a nondegenerate optical parametric amplifier (NOPA) is quite similar to that of the squeezed light with the DOPA. With cascaded NOPA (C-NOPA) [43,44] and feedback-controlled NOPA (CFC-NOPA) [45], the entanglement enhancement of lights has also been realized in experiments. However, the two schemes are mainly discussed separately, and few studies have compared their performance for enhancement of the quantum property. Thus far, experimenters are still confused about which scheme to choose. Recently, we noticed that Xin *et al.* compared the enhancement of quadrature entanglement with the C-NOPA and CFC-NOPA [46]. They concluded that CFC-NOPA has unique advantages over the C-NOPA. However, they adopted a simple model in which the analysis frequency was not considered. Therefore, their results are mainly responsible for zero analysis frequency, at which the squeezing is quite hard to observe in experiments due to some technique reasons. In this study, originating from the quantum Langevin equation, we obtained the complete noise formulas of the squeezed light from the C-DOPA and CFC-DOPA, depending on the analysis frequency. Using these formulas, the dependence of the noise variance of the light from the C-DOPA and CFC-DOPA on feasible physical parameters, including analysis frequency, pump parameters, and the loss of the system, is numerically simulated. Hence, the performance of the squeezing enhancement for the two cases is compared in detail.

2. THEORETICAL MODEL

A. Squeezed Light from a DOPA

First, we consider a DOPA shown in Fig. 1. All the mirrors are transparent to the pumping light. For the signal light, M2 has a power transmissivity of T_1, and the other mirrors are highly reflective. We assume that the intensity of the pump light is much larger than that of the signal light, and the quantum Langevin equation for the intracavity field $\hat{a}$ is given by

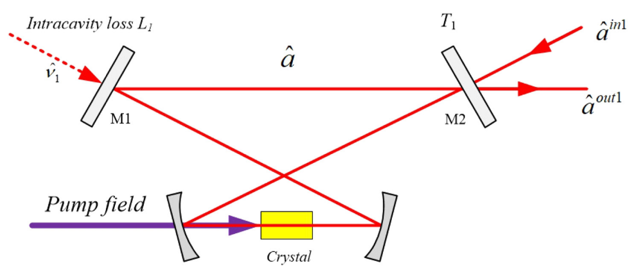

Fig. 1. Schematic of a DOPA.

$$\tau\dot{\hat{a}}(t) = -\frac{\gamma}{2}\hat{a}(t) \pm \kappa\hat{a}^{\dagger}(t) + \sqrt{T_1}\hat{a}^{in1}(t) + \sqrt{L_1}\hat{v}_1, \tag{1}$$

where τ is the round-trip time, L_1 is the intracavity loss, and $\gamma = T_1 + L_1$ represents the total loss of the cavity. κ represents the nonlinear coupling efficiency of the DOPA, which depends on the amplitude of the pump field and the second-order nonlinear coupling coefficient of the nonlinear crystal. $\hat{a}^{in1}$ is the injected signal field, and $\hat{v}_1$ is the vacuum field coupled with the intracavity loss. The sign $\pm$ denotes different modes of the DOPA, $+$ is the parametric amplification, and $-$ is the parametric deamplification.

Using the operator linearization method, in which the operators can be expressed by the sum of the mean value and the fluctuating component, that is, $\hat{a} = \alpha + \delta\hat{a}$, and then substituting the relationships, that is, $\delta\hat{X}_a = \delta\hat{a}^{\dagger} + \delta\hat{a}$ and $\delta\hat{Y}_a = i(\delta\hat{a}^{\dagger} - \delta\hat{a})$, we can obtain the equations of motion for the fluctuation of the quadratures of the light:

$$\tau\delta\dot{\hat{X}}_a(t) = -\frac{\gamma}{2}\delta\hat{X}_a(t) \pm \kappa\delta\hat{X}_a(t) + \sqrt{T_1}\delta\hat{X}_a^{in1}(t) + \sqrt{L_1}\delta\hat{X}_{v1}, \tag{2}$$

$$\tau\delta\dot{\hat{Y}}_a(t) = -\frac{\gamma}{2}\delta\hat{Y}_a(t) \mp \kappa\delta\hat{Y}_a(t) + \sqrt{T_1}\delta\hat{Y}_a^{in1}(t) + \sqrt{L_1}\delta\hat{Y}_{v1}. \tag{3}$$

For Eqs. (2) and (3), we first take the Fourier transform. Then, by introducing the input–output relation, that is, $\hat{a}^{\mathrm{out1}} = \sqrt{T_1}\hat{a} - \hat{a}^{\mathrm{in1}}$, the operator linearization method, and the relationships of the fluctuations of the quadrature operator and the creation and annihilation operators, we easily get $\delta\hat{X}_a^{\mathrm{out1}} = \sqrt{T_1}\delta\hat{X}_a - \delta\hat{X}_a^{\mathrm{in1}}$ and $\delta\hat{Y}_a^{\mathrm{out1}} = \sqrt{T_1}\delta\hat{Y}_a - \delta\hat{Y}_a^{\mathrm{in1}}$. With the relation, the fluctuation of the quadratures of the light from the DOPA can be obtained by

$$\delta\hat{X}_a^{\mathrm{out1}} = \frac{\left(\frac{T_1}{2} - \frac{L_1}{2} \pm \kappa - i\Omega\right)\delta\hat{X}_a^{\mathrm{in1}} + \sqrt{T_1 L_1}\delta\hat{X}_{v1}}{\frac{T_1}{2} + \frac{L_1}{2} \mp \kappa + i\Omega}, \tag{4}$$

$$\delta\hat{Y}_a^{\mathrm{out1}} = \frac{\left(\frac{T_1}{2} - \frac{L_1}{2} \mp \kappa - i\Omega\right)\delta\hat{Y}_a^{\mathrm{in1}} + \sqrt{T_1 L_1}\delta\hat{Y}_{v1}}{\frac{T_1}{2} + \frac{L_1}{2} \pm \kappa + i\Omega}, \tag{5}$$

where $\Omega = 2\pi f\tau$, and f is the analysis frequency. In addition, κ is related to the normalized pump parameter x using the formula $\kappa = x\gamma/2$. For simplicity, we denote

$$m_1 = \frac{\frac{T_1}{2} - \frac{L_1}{2} \pm \kappa - i\Omega}{\frac{T_1}{2} + \frac{L_1}{2} \mp \kappa + i\Omega}, \quad n_1 = \frac{\sqrt{T_1 L_1}}{\frac{T_1}{2} + \frac{L_1}{2} \mp \kappa + i\Omega}, \tag{6}$$

$$m_2 = \frac{\frac{T_1}{2} - \frac{L_1}{2} \mp \kappa - i\Omega}{\frac{T_1}{2} - \frac{L_1}{2} \pm \kappa + i\Omega}, \quad n_2 = \frac{\sqrt{T_1 L_1}}{\frac{T_1}{2} - \frac{L_1}{2} \pm \kappa + i\Omega}. \tag{7}$$

Then the fluctuation of quadratures of the light can be deduced as

$$\delta\hat{X}_a^{\mathrm{out1}} = m_1\delta\hat{X}_a^{\mathrm{in1}} + n_1\delta\hat{X}_{v1}, \; \delta\hat{Y}_a^{\mathrm{out1}} = m_2\delta\hat{Y}_a^{\mathrm{in1}} + n_2\delta\hat{Y}_{v1}. \tag{8}$$

In this study, we assume that the input signal field is a coherent or vacuum field, and the fluctuation variances are given by

$$\langle\delta^2\hat{X}_a^{\mathrm{out1}}\rangle = |m_1|^2 + |n_1|^2, \; \langle\delta^2\hat{Y}_a^{\mathrm{out1}}\rangle = |m_2|^2 + |n_2|^2. \tag{9}$$

It can be seen from the equation that the DOPA produces the quadrature amplitude squeezed light in the deamplification mode, while it generates the quadrature phase squeezed light in the amplification mode. In our discussion, we assume that the DOPA is run in the deamplification mode, that is, the sign $\pm$ is set to $-$, and $\langle\delta^2\hat{X}_a^{\mathrm{out1}}\rangle < 1$.

B. Squeezed Light from a CFC-DOPA

Next, we discuss a CFC-DOPA, which is depicted in Fig. 2. In the CFC loop, a beam splitter (BS) with tunable transmissivity T_2 plays the roles of both a controller and an input–output port, which is called control-BS (CBS). Note that a realistic model corresponding to an actually constructed optical system in the laboratory, which considers both the time delay and propagation loss in the feedback loop, is studied. The propagation loss for the CFC loop can be modeled as an unwanted vacuum field $\hat{v}_2$ coupled from a lossy mirror with transmissivity L_2. The total phase delay introduced by the CFC loop is denoted by ϕ. The injected signal field $\hat{c}^{\mathrm{in}}$ was injected into the DOPA through the CBS. Subsequently, the output field $\hat{a}^{\mathrm{out1}}$ is reflected by the lossy mirror M, and then the reflected field $\hat{b}^{\mathrm{in}}$ is sent to one port of the CBS. One output of CBS $\hat{b}^{\mathrm{out}}$ is sent back to the DOPA after phase delay ϕ. At the other port of the CBS, we obtain an enhanced squeezed field $\hat{c}^{\mathrm{out}}$. The input–output relationship of the CBS is given by

$$\hat{b}^{\mathrm{out}}(t) = \sqrt{T_2}\hat{c}^{\mathrm{in}}(t) + \sqrt{1 - T_2}\hat{b}^{\mathrm{in}}(t), \tag{10}$$

$$\hat{c}^{\mathrm{out}}(t) = \sqrt{T_2}\hat{b}^{\mathrm{in}}(t) - \sqrt{1 - T_2}\hat{c}^{\mathrm{in}}(t). \tag{11}$$

At the mirror M, we have

$$\hat{b}^{\mathrm{in}}(t) = \sqrt{1 - L_2}\hat{a}^{\mathrm{out1}}(t) + \sqrt{L_2}\hat{v}_2(t). \tag{12}$$

Considering the phase delay ϕ, we obtain

$$\hat{a}^{\mathrm{in1}}(t) = \hat{b}^{\mathrm{out}}(t)e^{i\phi}. \tag{13}$$

To obtain the input–output relation of the CFC-DOPA in terms of the quadrature representation, for Eqs. (10)–(13), we also use the operator linearization method and substitute the relationships, that is, $\delta\hat{X}_k = \delta\hat{k}^{\dagger} + \delta\hat{k}$ and $\delta\hat{Y}_k = i(\delta\hat{k}^{\dagger} - \delta\hat{k})$ with $k = a, b, c, v_1, v_2$. Subsequently, taking the Fourier transform of these equations and eliminating the intermediate operators by combining with Eq. (8), we obtain

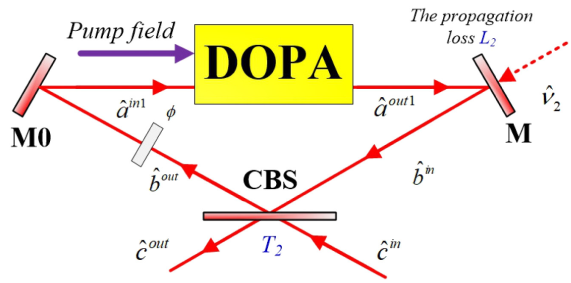

Fig. 2. Schematic of a CFC-DOPA.

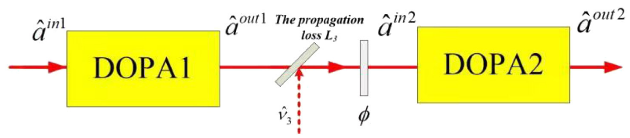

Fig. 3. Schematic of a C-DOPA.

$$\delta\hat{X}_c^{\text{out}} = -\left(\sqrt{1-T_2} - \frac{m_1 A T_2\sqrt{1-L_2}}{B}\right)\delta\hat{X}_c^{\text{in}}$$
$$\times\left[n_1\sqrt{T_2}\sqrt{1-L_2} + \frac{m_1 n_1 A\sqrt{T_2}\sqrt{1-T_2}(1-L_2)}{B}\right]\delta\hat{X}_{v1} + \left(\sqrt{T_2 L_2} + \frac{m_1 A\sqrt{T_2}\sqrt{1-T_2}\sqrt{L_2}\sqrt{1-L_2}}{B}\right)\delta\hat{X}_{v2}$$
$$-\frac{\sqrt{T_2}\sqrt{1-L_2}m_1\sin\phi}{B}\left(\sqrt{T_2}\delta\hat{Y}_c^{\text{in}} + n_2\sqrt{1-T_2}\sqrt{1-L_2}\delta\hat{Y}_{v1} + \sqrt{1-T_2}\sqrt{L_2}\delta\hat{Y}_{v2}\right), \tag{14}$$

where

$$A = \cos\phi - \sqrt{1-T_2}\sqrt{1-L_2}m_2, \tag{15}$$

$$B = 1 - \sqrt{1-T_2}\sqrt{1-L_2}\,(m_1+m_2)\cos\phi + (1-T_2)(1-L_2)m_1 m_2. \tag{16}$$

Then, the fluctuation variance is given by

$$\left\langle\delta^2\hat{X}_c^{\text{out}}\right\rangle = \left|\sqrt{1-T_2} - \frac{m_1 A T_2\sqrt{1-L_2}}{B}\right|^2$$
$$+\left|n_1\sqrt{T_2}\sqrt{1-L_2} + \frac{m_1 n_1 A\sqrt{T_2}\sqrt{1-T_2}(1-L_2)}{B}\right|^2$$
$$+\left|\sqrt{T_2 L_2} + \frac{m_1 A\sqrt{T_2}\sqrt{1-T_2}\sqrt{L_2}\sqrt{1-L_2}}{B}\right|^2$$
$$+\left|\frac{\sqrt{T_2}\sqrt{1-L_2}m_1\sin\phi}{B}\right|^2$$
$$\times\left[T_2 + n_2^2(1-T_2)(1-L_2) + (1-T_2)L_2\right]. \tag{17}$$

C. Squeezed Light from a C-DOPA

Finally, we consider a C-DOPA as depicted in Fig. 3. To simplify the calculation, we assume that the two DOPAs are identical; hence, the intracavity loss and power transmissivity of the output coupler for the second DOPA are also denoted as L_1 and T_1, respectively. The propagation loss from the output of DOPA1 to the input of DOPA2 can be modeled as an unwanted vacuum noise $\hat{v}_3$ coupled from a lossy mirror with reflectivity L_3. The phase delay is denoted by ϕ. Then the output of DOPA1 and the input of DOPA2 are related as

$$\hat{a}^{\text{in}2}(t) = \left(\sqrt{1-L_3}\hat{a}^{\text{out}1}(t) + \sqrt{L_3}\hat{v}_3(t)\right)e^{i\phi}. \tag{18}$$

Using the same procedure as the calculation of noise variance for the single DOPA and CFC-DOPA, we can easily obtain

$$\delta^2\hat{X}_a^{\text{in}2} = (1-L_3)\left(\cos^2\phi\,\delta^2\hat{X}_a^{\text{out}1} + \sin^2\phi\,\delta^2\hat{Y}_a^{\text{out}1}\right) + L_3. \tag{19}$$

For DOPA2, we have

$$\delta^2\hat{X}_a^{\text{out}2} = |m_1|^2\delta^2\hat{X}_a^{in2} + |n_1|^2\delta^2\hat{X}_{v4}, \tag{20}$$

where $\hat{v}_4$ is the vacuum field coupled with the intracavity loss for DOPA2. Substituting Eq. (9), the fluctuation variance of the light produced by the C-DOPA is obtained by

$$\delta^2\hat{X}_a^{\text{out}2} = |m_1|^2(1-L_3)$$
$$\left[\cos^2\phi(|m_1|^2+|n_1|^2) + \sin^2\phi\left(|m_2|^2+|n_2|^2\right)\right]$$
$$+|m_1|^2 L_3 + |n_1|^2. \tag{21}$$

3. RESULTS AND DISCUSSION

A. Squeezing with Ideal Parameters

We first discuss the noise performance of the squeezed light produced by the DOPA, C-DOPA, and CFC-DOPA for an ideal case, in which all the losses of the system are ruled out and the analysis frequency is zero, that is, $L_1 = L_2 = L_3 = 0$ and $f = 0$. For the CFC-DOPA, we can infer from Eq. (17) that $\phi = 0$ denotes positive feedback, for which the squeezing level produced by CFC-DOPA can be enhanced for a certain region of the CBS transmissivity T_2. We plotted the squeezing degree of the light output from the CFC-DOPA versus T_2 at a moderate pump parameter $x = 0.4$ and $\phi = 0$ as shown in Fig. 4(a). The results for the single DOPA are also plotted for comparison. The behavior of the curve can be understood by considering the trade-off between the enhancement of the squeezing effect and the loss of the CFC loop. The reflected squeezed light by CBS feeds back to the DOPA, leading to the enhancement of squeezing via nonlinear interaction, while the loss of the CFC loop degrades the squeezing. The loss of the CFC loop here refers to the reflection loss induced by the CBS. When $T_2 < 0.475$, the loss is dominant, causing a smaller squeezing degree compared with that of the single DOPA. With an increase in T_2, the loss of the CBS is reduced significantly. After $T_2 > 0.475$, the enhancement of the squeezing effect tends to be dominant, leading to an enhanced squeezing level. In this region, an optimal transmissivity can be found to provide a maximum degree of squeezing. For the ideal case, Eq. (17)

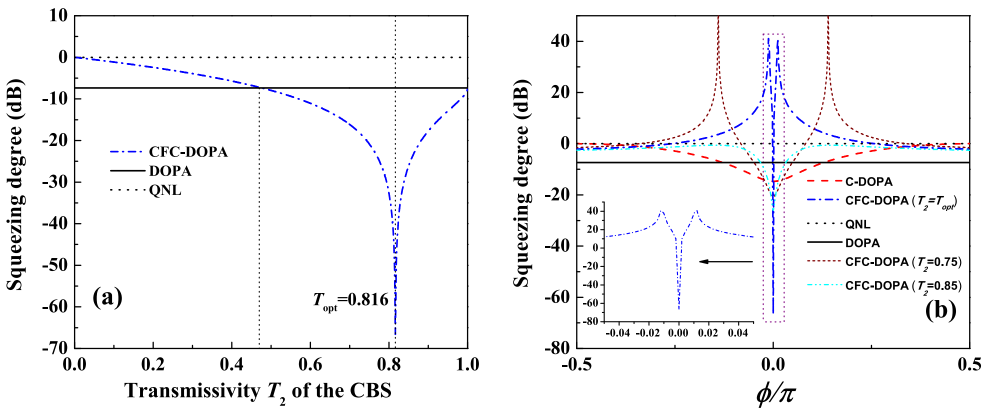

Fig. 4. (a) Dependence of squeezing degree on the transmissivity T_2 of the CBS for the CFC-DOPA, for the ideal case; (b) dependence of squeezing degree on the phase ϕ for the squeezed states generated from the CFC-DOPA, C-DOPA, and single DOPA, for the ideal case. The common parameters used in the figures are as follows: (a) $L_1 = L_2 = L_3 = 0$, $f = 0$, and $x = 0.4$. $\phi = 0$ and (b) $T_2 = T_{opt} = 0.816$.

can be easily simplified, and the optimal transmissivity of the CBS is given by $T_{opt} = 1 - (1 - x)^2/(1 + x)^2$. For $x = 0.4$, the maximum squeezing is achieved at $T_{opt} = 0.816$.

The dependence of the squeezing degree on the phase ϕ from the CFC-DOPA, C-DOPA, and DOPA is also plotted at $x = 0.4$ as shown in Fig. 4(b). The curve for the CFC-DOPA was simulated at $T_2 = T_{opt} = 0.816$, $T_2 = 0.75$, and $T_2 = 0.85$; the result for the C-DOPA was simulated using Eq. (21). From the figure, we can infer that both the C-DOPA and CFC-DOPA can enhance the squeezing of the single DOPA by manipulating the phase delay. Furthermore, we are surprised that the output squeezing for the CFC-DOPA at a fixed pump parameter can be infinity by manipulating the transmissivity T_2 of the CBS. However, it requires almost infinity accuracy in phase locking as shown in the inset of Fig. 4(b). It also can be seen from the figure that when T_2 slightly deviates from T_{opt}, the squeezing of CFC-DOPA weakens, but it is still advantageous over the DOPA and C-DOPA within a phase region. There exists a trade-off between squeezing enhancement and the phase region where the squeezing generated from the CFC-DOPA is enhanced compared with that from the single DOPA.

B. Squeezing with Practical Experimental Parameters

The results discussed above seem interesting and instructive, but they can only be realized under strict experimental parameters. To provide useful references for practical system designs, we further studied a system with experimentally reachable parameters, in which the intracavity loss of the DOPA and the propagation loss were considered. To simplify the discussion without losing generality, we assumed that the propagation losses for the CFC-DOPA and C-DOPA are equal, that is, $L_2 = L_3$. Furthermore, as the intensity and phase noise of both the pump and signal laser are quite strong around zero frequency, we set an analysis frequency of 2 MHz, at which the noise of the light can reach the quantum noise limit after the filtering of the mode cleaner. The values of the parameters used in the calculation are as follows: the loss of the DOPA cavity $L_1 = 0.005$, transmissivity of the output coupler of the DOPA cavity $T_1 = 0.12$, round-trip time $\tau = 2 \times 10^{-9}$ s, propagation loss $L_2 = L_3 = 0.01$, analysis frequency $f = 2$ MHz, and pump parameter $x = 0.4$. The parameters of the DOPA cavity are consistent with our previously published paper on the generation of squeezed light at 795 nm [33]. The dependence of the squeezing degree versus the transmissivity T_2 of the CBS for $\phi = 0$ is also plotted in Fig. 5(a). The behavior and physical mechanism are roughly the same as the ideal case discussed above. The only difference is that the loss here includes not only the loss of CBS but also the propagation loss and the intracavity loss of the DOPA cavity. As a result, the critical T_2 at which the curves of the CFC-DOPA and DOPA intersect as well as the optimal transmissivity T_{opt} tend to a larger value. For this case, Eq. (17) is relatively complex, and it is difficult to obtain an analytical solution. For a set of given system parameters, one can find the transmissivity range of the squeezing enhancement and T_{opt} by numerical simulation based on Eq. (17). For the present parameters, the optimal transmissivity of $T_{opt} = 0.946$ was obtained.

The dependence of the squeezing degree on the phase ϕ with the mentioned parameters for the CFC-DOPA, C-DOPA, and single DOPA is plotted for comparison in Fig. 5(b). The results for the CFC-DOPA were simulated at $T_{opt} = 0.946$. From the figure, we can infer that the CFC-DOPA and C-DOPA can also enhance the squeezing output from the single DOPA for the lossy case. However, the C-DOPA is advantageous for the enhancement of squeezing. This shows a different conclusion compared to that in Ref. [46]. The essential reason for this is that the analysis frequency was not included in their model. Therefore, their conclusion is responsible for the zero frequency. As discussed above, the experimental realization of quadrature squeezed light at zero frequency is still hard for now. Therefore, we believe that the conclusion obtained here with an experimental measurable analysis frequency is a valuable reference. In addition, we define R_E as the phase region where the squeezing generated from the C-DOPA and CFC-DOPA is enhanced compared with that from the single DOPA, as shown in Fig. 5(b), with $R_E < 2\pi$. R_E is another important physical quantity for judging the practicability of phase-sensitive amplifiers, denoting instability tolerance in phase locking. From Fig. 5(b), we notice that the C-DOPA shows the advantage of enhancement of squeezing but no advantage with respect to R_E.

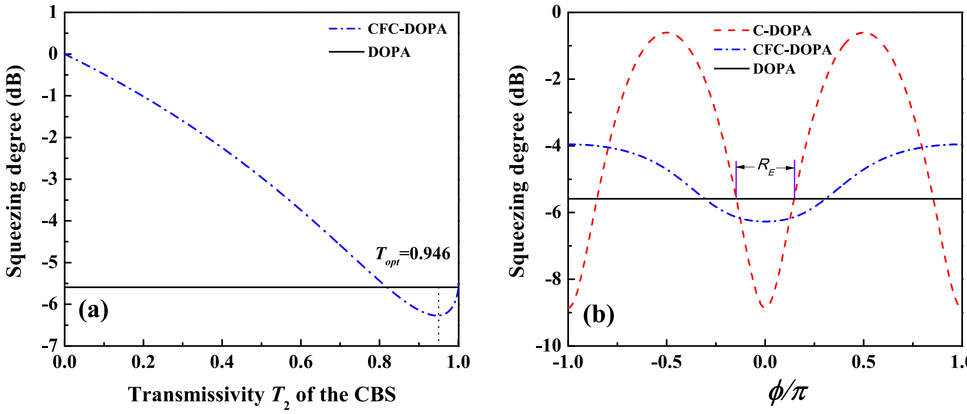

Fig. 5. (a) Dependence of squeezing degree on the transmissivity T_2 of the CBS for the CFC-DOPA, for the lossy case; (b) dependence of squeezing degree on the phase ϕ for the squeezed states generated from the CFC-DOPA, C-DOPA, and single DOPA, for the lossy case. The common parameters used in the figures are as follows: (a) $L_1 = 0.005$, $L_2 = L_3 = 0.01$, $T_1 = 0.12$, $\tau = 2 \times 10^{-9}s$, $f = 2$ MHz, $x = 0.4$. $\phi = 0$ and (b) $T_2 = T_{\rm opt} = 0.946$.

The above discussion focuses on a specific analysis frequency. To ensure the generality of the discussion, the spectrum distribution of the squeezing degree for the CFC-DOPA, C-DOPA, and single DOPA is plotted and compared as shown in Fig. 6. The parameters are similar to those used in Fig. 5, and $\phi = 0$ was chosen. The dependence of $T_{\rm opt}$ on the analysis frequency f is shown in the inset. Note that the result of the CFC-DOPA is obtained at $T_{\rm opt}$ for each frequency. As shown in Fig. 6, the squeezing is enhanced by the CFC-DOPA when $f < 3.3$ MHz. The maximum enhancement for the squeezing occurs at zero frequency, and the enhancement decreases with an increase in f. After $f > 3.3$ MHz, the squeezing tends to be slightly weaker than that of the single DOPA. This is mainly induced by the delay of the feedback loop, which affects the control performance and operation bandwidth of the CFC-DOPA. This is quite similar to the feedback control in electronics, in which positive feedback increases gain at the expense of bandwidth. In stark contrast, the CFC-DOPA can realize almost a broadband enhancement of squeezing in the frequency range of $0 - 5$ MHz. Comparing the curves of the CFC-DOPA and C-DOPA, it can be seen that the CFC-DOPA can produce a higher squeezing degree when $f < 0.44$ MHz. This result presents a more general frequency range, at which the CFC-DOPA indicates the advantage of squeezing enhancement compared with Ref. [46] fixed at zero frequency. After $f > 0.44$ MHz, the C-DOPA shows an advantage in the enhancement of squeezing, and the advantage strengthens as f increases. Compared with the advantage of the C-DOPA in the megahertz range, the advantage of the CFC-DOPA in the low-frequency band is inconspicuous. In addition, the realization of quadrature squeezed light with the DOPA in the low-frequency range is still difficult as the noise of the laser and electronic loop increases. Therefore, the following discussion is fixed at a general analysis frequency of 2 MHz.

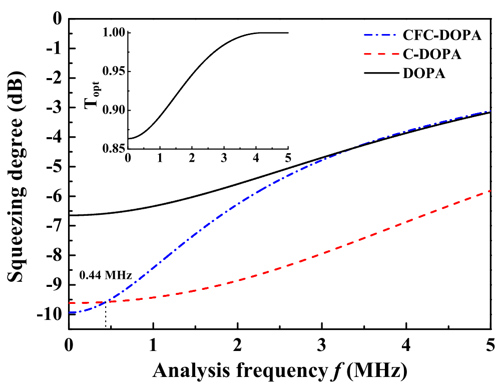

Fig. 6. Dependence of squeezing degree on the analysis frequency. The parameters used in the figures are as follows: $L_1 = 0.005$, $L_2 = L_3 = 0.01$, $T_1 = 0.12$, $\tau = 2 \times 10^{-9}$ s, $x = 0.4$, and $\phi = 0$.

To further expand the generality of the discussion, the dependence of the squeezing degree on the pump parameters at $f = 2$ MHz is plotted in Fig. 7. The corresponding $T_{\rm opt}$ versus pump parameter x is shown in the inset. The squeezing degree for each pump parameter was optimized to be that at $T_{\rm opt}$. First, we compare the curves of the single DOPA and CFC-DOPA. This behavior can also be explained by considering the trade-off between the enhancement of the squeezing effect and loss of the CFC loop. When $x < 0.64$, the enhancement of the squeezing effect is dominant, and thus the CFC-DOPA can enhance the squeezing of the single DOPA. The squeezing produced by the single DOPA strengthens with an increase in x. Squeezing is quite sensitive to the loss. The higher the squeezing, the stronger the degradation induced by loss. As x increases, the effect of the loss significantly strengthens and becomes dominant, resulting in the fact that the squeezing output from the CFC-DOPA is weaker than that of the single DOPA after $x > 0.64$. From the curve of the C-DOPA, it can be seen that the C-DOPA can realize the enhancement of squeezing for all ranges of x, and the squeezing level obtained by the C-DOPA is always stronger than that of the CFC-COPA. From this point of view, the C-DOPA also shows an obvious advantage compared with the CFC-DOPA.

In the following, we discuss the robustness of the C-DOPA and CFC-DOPA against the loss of the system. The squeezing level produced by the C-DOPA and CFC-DOPA versus intracavity loss L_1 and propagation loss $L_2(L_3)$ are plotted as shown in Figs. 8(a) and 9(a), respectively. The results for the

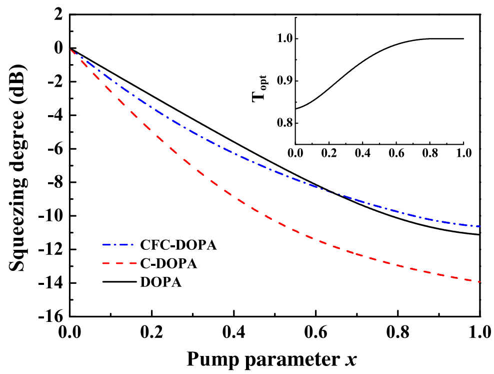

Fig. 7. Dependence of squeezing degree on the pump parameter x. The parameters used in the figures are as follows: $L_1 = 0.005$, $L_2 = L_3 = 0.01$, $T_1 = 0.12$, $\tau = 2 \times 10^{-9} s$, $\phi = 0$, and $f = 2$ MHz.

single DOPA are also plotted for comparison. The insets show T_{opt} versus L_1 and $L_2(L_3)$. The common parameters used in the two figures are as follows: $x = 0.4$, $\tau = 2 \times 10^{-9} s$, $\phi = 0$, $T = T_{\text{opt}}$, and $f = 2$ MHz. In Fig. 8, we set $L_2(L_3) = 0.01$ and numerically simulated results for a practical intracavity loss range of $0 < L_1 < 0.02$. For Fig. 9, we set $L_1 = 0.005$ and obtained results for a practical propagation loss range of $0 < L_2(L_3) < 0.04$. From the two figures, we can conclude that both the CFC-DOPA and C-DOPA can enhance the squeezing for the practical loss range. With an increase in L_1, the squeezing produced by both the CFC-DOPA and C-DOPA degrades remarkably, and the result for the CFC-DOPA is always better than that of the C-DOPA. As $L_2(L_3)$ increases, the degradation of squeezing for the CFC-DOPA is more serious than that of the C-DOPA. This implies that the squeezing produced by the CFC-DOPA is more sensitive to the propagation loss. Based on the above discussion, the C-DOPA retains the advantage of squeezing enhancement and shows better robustness against loss. The squeezing enhancement region R_E of the C-DOPA and CFC-DOPA versus the loss is also shown in Figs. 8(b) and 9(b). As the price of advantage on the squeezing enhancement, the R_E of the C-DOPA is always smaller than that of the CFC-DOPA for the practical loss range. This denotes a smaller instability tolerance and may require a slightly higher accuracy in phase locking.

Note that the squeezing discussed above is the direct output from the single DOPA, C-DOPA, and CFC-DODA. With the following parameters: $L_1 = 0.005$, $T_1 = 0.12$, $\tau = 2 \times 10^{-9} s$, $L_2 = L_3 = 0.01$, $f = 2$ MHz, and $x = 0.4$, -5.59 dB of the quadrature squeezed light can be directly obtained from the single DOPA. For the C-DOPA, -8.86 dB of squeezing can

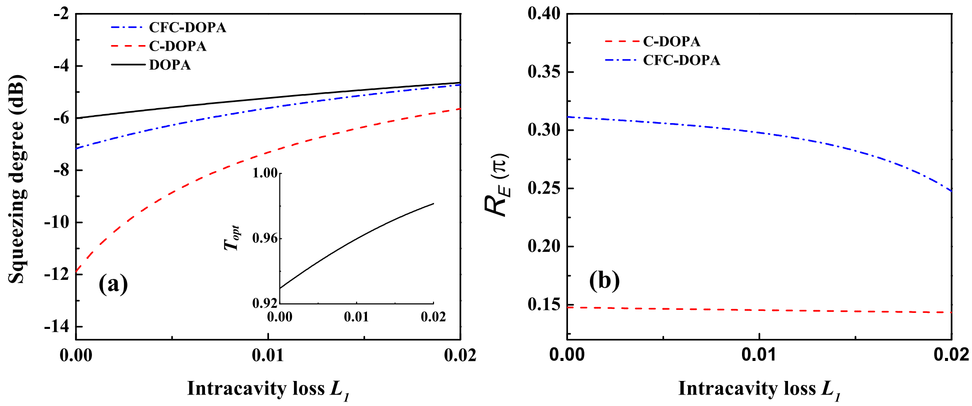

Fig. 8. Dependence of (a) squeezing degree and (b) R_E on the intracavity loss L_1 for the squeezed states generated from the CFC-DOPA, C-DOPA, and single DOPA. The parameters used in the figures are as follows: $L_2 = L_3 = 0.01$, $T_1 = 0.12$, $\tau = 2 \times 10^{-9}$ s, $x = 0.4$, $\phi = 0$, and $f = 2$ MHz.

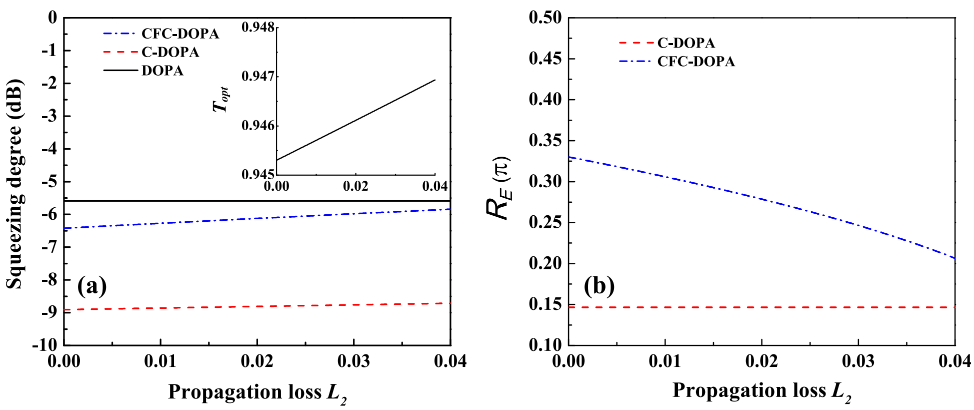

Fig. 9. Dependence of (a) squeezing degree and (b) R_E on the propagation loss L_2 for the squeezed states generated from the CFC-DOPA, C-DOPA, and single DOPA. The parameters used in the figures are as follows: $L_1 = 0.005$, $T_1 = 0.12$, $\tau = 2 \times 10^{-9}$ s, $x = 0.4$, $\phi = 0$, and $f = 2$ MHz.

be expected at $\phi = 0$, while -6.27 dB of squeezing can be produced by the CFC-DOPA at $T = T_{\mathrm{opt}}$ and $\phi = 0$. However, the actual measured squeezing in experiments should consider the detection efficiency, which includes the homodyne visibility, the quantum efficiency of the photodiodes, and the propagation loss from the squeezing source to the detection system. Considering the practical detection efficiency of 93% [32,33], the measurable squeezing becomes -4.86 dB, -5.38 dB, and -7.19 dB for the single DOPA, CFC-DOPA, and C-DOPA, respectively. The calculated result for the single DOPA with feasible physical parameters of realistic systems matches the observed results in experiments [32,33]. The C-DOPA has the potential to push the squeezing level of the quadrature squeezed light at 795 nm to be better than -7 dB. In the future, we believe that the fabrication technology for nonlinear crystals will be further improved. We hope that one day the crystals can be exposured to high violet power without the loss increase and damage. Thereafter, the DOPA on the production of squeezed light at 795 nm can be operated at a higher pump parameter. As shown in Fig. 7, when the DOPA is run at a pump parameter of $x = 0.7$, a measurable squeezing level of -10 dB with the C-DOPA can be expected.

4. CONCLUSION

In summary, the performance of the squeezing enhancement for the C-DOPA and CFC-DOPA is compared in detail. For the ideal case, the squeezing level produced by the CFC-DOPA can be infinitely larger at a fixed pump parameter. However, for a practical case with the feasible loss and analysis megahertz frequency range, the C-DOPA shows an obvious advantage in the enhancement of the squeezing level. The CFC-DOPA shows a slight advantage in the low-frequency range. Furthermore, the C-DOPA can realize a broadband squeezing enhancement for all ranges of pump parameters, while the CFC-DOPA can only enhance the squeezing level of the single DOPA for a narrow bandwidth and a limited pump parameter range. In addition, the C-DOPA showed better robustness against loss. The only disadvantage inferred from our simulation for the C-DOPA is that it requires a smaller instability tolerance, for which special care of phase locking should be taken in actual experiments. In consideration of experimental realization, the other disadvantage for C-DOPA may be that the device is a little cumbersome compared with the CFC-DOPA. For practical experiments, it is necessary to balance these advantages and disadvantages.

Although our analysis is based on the parameters used in the production of squeezed light at 795 nm, the wavelengths of other atomic transitions are also near infrared or visible bands, which may face similar difficulties in the production of high-quality squeezed light. Therefore, our results can provide an important reference for improving the squeezing level of squeezed and entangled light at short wavelengths, especially for wavelengths corresponding to atomic transitions, which have great potential applications in future quantum information processing and quantum metrology. Furthermore, it can also contribute to a deeper understanding of the DOPA, C-DOPA, and CFC-DOPA.

Funding. National Natural Science Foundation of China (12104013, 12074005, 11974226, 61875111); Key Program of Innovation and Entrepreneurship Support Plan for Returned Talents in Anhui Province (2020LCX007); Natural Science Research Projects of the Universities in Anhui Province (KJ2020A0052), Anhui Province Key Laboratory of Optoelectric Materials Science and Technology (OMST202107).

Acknowledgment. Y. H. thanks Dr. Hidehiro Yonezawa for helpful discussions.

Disclosures. The authors declare no conflicts of interest.

Data Availability. Data underlying the results presented in this paper are not publicly available at this time but may be obtained from the authors upon reasonable request.

REFERENCES

1. S. L. Braunstein and P. van Loock, "Quantum information with continuous variables," Rev. Mod. Phys. **77**, 513–577 (2005).
2. H. Zhong, H. Wang, and Y. Deng, *et al.*, "Quantum computational advantage using photons," Science **370**, 1460–1463 (2020).
3. X. Su, S. Hao, X. Deng, L. Ma, M. Wang, X. Jia, C. Xie, and K. Peng, "Gate sequence for continuous variable one-way quantum computation," Nat. Commun. **4**, 2828 (2013).
4. B. Li, J. Bílek, U. B. Hoff, L. S. Madsen, S. Forstner, V. Prakash, C. Schäfermeier, T. Gehring, W. P. Bowen, and U. L. Andersen, "Quantum enhanced optomechanical magnetometry," Optica **5**, 850–856 (2018).
5. M. Tse, H. Yu, and N. Kijbunchoo, *et al.*, "Quantum-enhanced advanced LIGO detectors in the era of gravitational-wave astronomy," Phys. Rev. Lett. **123**, 231107 (2019).
6. R. E. Slusher, L. W. Hollberg, B. Yurke, J. C. Mertz, and J. F. Valley, "Observation of squeezed states generated by four-wave mixing in an optical cavity," Phys. Rev. Lett. **55**, 2409–2412 (1985).
7. N. V. Corzo, Q. Glorieux, A. M. Marino, J. B. Clark, R. T. Glasser, and P. D. Lett, "Rotation of the noise ellipse for squeezed vacuum light generated via four-wave mixing," Phys. Rev. A **88**, 043836 (2013).
8. S. Kim and A. M. Marino, "Atomic resonant single-mode squeezed light from four-wave mixing through feedforward," Opt. Lett. **44**, 4630–4633 (2019).
9. S. Kim and A. M. Marino, "Generation of ^{87}Rb resonant bright two-mode squeezed light with four-wave mixing," Opt. Express **26**, 33366–33375 (2018).
10. L.-A. Wu, H. J. Kimble, J. L. Hall, and H. Wu, "Generation of squeezed states by parametric down conversion," Phys. Rev. Lett. **57**, 2520–2523 (1986).
11. M. Mehmet, S. Ast, T. Eberle, S. Steinlechner, H. Vahlbruch, and R. Schnabel, "Squeezed light at 1550 nm with a quantum noise reduction of 12.3 dB," Opt. Express **19**, 25763–25772 (2011).
12. H. Vahlbruch, M. Mehmet, K. Danzmann, and R. Schnabel, "Detection of 15 dB squeezed states of light and their application for the absolute calibration of photoelectric quantum efficiency," Phys. Rev. Lett. **117**, 110801 (2016).
13. A. Schönbeck, F. Thies, and R. Schnabel, "13 dB squeezed vacuum states at 1550 nm from 12 mW external pump power at 775 nm," Opt. Lett. **43**, 110–113 (2018).
14. W. Zhang, J. Wang, Y. Zheng, Y. Wang, and K. Peng, "Optimization of the squeezing factor by temperature-dependent phase shift compensation in a doubly resonant optical parametric oscillator," Appl. Phys. Lett. **115**, 171103 (2019).
15. J. Heersink, T. Gaber, S. Lorenz, O. Glöckl, N. Korolkova, and G. Leuchs, "Polarization squeezing of intense pulses with a fiber-optic Sagnac interferometer," Phys. Rev. A **68**, 013815 (2003).
16. J. Heersink, V. Josse, G. Leuchs, and U. L. Andersen, "Efficient polarization squeezing in optical fibers," Opt. Lett. **30**, 1192–1194 (2005).
17. Z. Yan, L. Wu, X. Jia, Y. Liu, R. Deng, S. Li, H. Wang, C. Xie, and K. Peng, "Establishing and storing of deterministic quantum entanglement among three distant atomic ensembles," Nat. Commun. **8**, 718 (2017).
18. V. G. Lucivero, R. Jiménez-Martínez, J. Kong, and M. W. Mitchell, "Squeezed-light spin noise spectroscopy," Phys. Rev. A **93**, 053802 (2016).

19. V. G. Lucivero, A. Dimic, J. Kong, R. Jiménez-Martínez, and M. W. Mitchell, "Sensitivity, quantum limits, and quantum enhancement of noise spectroscopies," Phys. Rev. A **95**, 041803 (2017).
20. F. Wolfgramm, A. Cerè, F. A. Beduini, A. Predojević, M. Koschorreck, and M. W. Mitchell, "Squeezed-light optical magnetometry," Phys. Rev. Lett. **105**, 053601 (2010).
21. F. McCormick, A. M. Marino, V. Boyer, and P. D. Lett, "Strong low-frequency quantum correlations from a four-wave-mixing amplifier," Phys. Rev. A **78**, 043816 (2008).
22. R. Pooser, A. Marino, V. Boyer, K. Jones, and P. D. Lett, "Quantum correlated light beams from non-degenerate four-wave mixing in an atomic vapor: the D_1 and D_2 lines of ^{58}Rb and ^{87}Rb," Opt. Express **17**, 16722–16730 (2009).
23. Q. Glorieux, L. Guidoni, S. Guibal, J.-P. Likforman, and T. Coudreau, "Strong quantum correlations in four wave mixing in ^{85}Rb vapor," Proc. SPIE **7727**, 772703 (2010).
24. R. Ma, W. Liu, Z. Qin, X. Jia, and J. Gao, "Generating quantum correlated twin beams by four-wave mixing in hot cesium vapor," Phys. Rev. A **96**, 043843 (2017).
25. J. Ries, B. Brezger, and A. I. Lvovsky, "Experimental vacuum squeezing in rubidium vapor via self-rotation," Phys. Rev. A **68**, 025801 (2003).
26. S. Barreiro, P. Valente, H. Failache, and A. Lezama, "Polarization squeezing of light by single passage through an atomic vapor," Phys. Rev. A **84**, 033851 (2011).
27. I. H. Agha, G. Messin, and P. Grangier, "Generation of pulsed and continuous-wave squeezed light with ^{87}Rb vapor," Opt. Express **18**, 4198–4205 (2010).
28. Y. Takeno, M. Yukawa, H. Yonezawa, and A. Furusawa, "Observation of -9 dB quadrature squeezing with improvement of phase stability in homodyne measurement," Opt. Express **15**, 4321–4327 (2007).
29. S. Burks, J. Ortalo, A. Chiummo, X. Jia, F. Villa, A. Bramati, J. Laurat, and E. Giacobino, "Vacuum squeezed light for atomic memories at the D_2 cesium line," Opt. Express **17**, 3777–3781 (2009).
30. J. Tian, G. Zuo, Y. Zhang, G. Li, P. Zhang, and T. Zhang, "Generation of squeezed vacuum on cesium D_2 line down to kilohertz range," Chin. Phy. B **26**, 124206 (2017).
31. T. Tanimura, D. Akamatsu, Y. Yokoi, A. Furusawa, and M. Kozuma, "Generation of a squeezed vacuum resonant on a rubidium D_1 line with periodically poled $KTiOPO_4$," Opt. Lett. **31**, 2344–2346 (2006).
32. G. Hétet, O. Glöckl, K. A. Pilypas, C. C. Harb, B. C. Buchler, H.-A. Bachor, and P. K. Lam, "Squeezed light for bandwidth-limited atom optics experiments at the rubidium D_1 line," J. Phys. B **40**, 221–226 (2007).
33. Y. Han, X. Wen, J. He, B. Yang, Y. Wang, and J. Wang, "Improvement of vacuum squeezing resonant on the rubidium D_1 line at 795 nm," Opt. Express **24**, 2350–2359 (2016).
34. S. Wang, V. Pasiskevicius, and F. Laurell, "Dynamics of green light-induced infrared absorption in $KTiOPO_4$ and periodically poled $KTiOPO_4$," J. Appl. Phys. **96**, 2023–2028 (2004).
35. B. Boulanger, I. Rousseau, J. P. Fève, M. Maglione, B. Ménaert, and G. Marnier, "Optical studies of laser-induced gray-tracking in KTP," IEEE J. Quantum Electron. **35**, 281–286 (1999).
36. K. McKenzie, E. E. Mikhailov, K. Goda, P. K. Lam, N. Grosse, M. B. Gray, N. Mavalvala, and D. E. McClelland, "Quantum noise locking," J. Opt. B **7**, S421–S428 (2005).
37. J. Zhang, C. Ye, F. Gao, and M. Xiao, "Phase-sensitive manipulations of a squeezed vacuum field in an optical parametric amplifier inside an optical cavity," Phys. Rev. Lett. **101**, 233602 (2008).
38. D. Wang, Y. Zhang, and M. Xiao, "Quantum limits for cascaded optical parametric amplifiers," Phys. Rev. A **87**, 023834 (2013).
39. J. E. Gough and S. Wildfeuer, "Enhancement of field squeezing using coherent feedback," Phys. Rev. A **80**, 042107 (2009).
40. J. E. Gough, M. R. James, and H. I. Nurdin, "Squeezing components in linear quantum feedback networks," Phys. Rev. A **81**, 023804 (2010).
41. O. Crisafulli, N. Tezak, D. B. S. Soh, M. A. Armen, and H. Mabuchi, "Squeezed light in an optical parametric oscillator network with coherent feedback quantum control," Opt. Express **21**, 18371–18376 (2013).
42. S. Iida, M. Yukawa, H. Yonezawa, N. Yamamoto, and A. Furusawa, "Experimental demonstration of coherent feedback control on optical field squeezing," IEEE Trans. Autom. Control **57**, 2045–2050 (2012).
43. Y. Shang, X. Jia, Y. Shen, C. Xie, and K. Peng, "Continuous variable entanglement enhancement and manipulation by a subthreshold type II optical parametric amplifier," Opt. Lett. **35**, 853–855 (2010).
44. Z. Yan, X. Jia, X. Su, Z. Duan, C. Xie, and K. Peng, "Cascaded entanglement enhancement," Phys. Rev. A **85**, 040305 (2012).
45. Y. Zhou, X. Jia, F. Li, J. Yu, C. Xie, and K. Peng, "Quantum coherent feedback control for generation system of optical entangled state," Sci. Rep. **5**, 11132 (2015).
46. J. Xin, X. Pan, X. Lu, J. Kong, G. Li, and X. Li, "Entanglement enhancement from a two-port feedback optical parametric amplifier," Phys. Rev. Appl. **14**, 024015 (2020).